Indian Journal of Engineering & Materials Sciences
Vol. 27, August 2020, pp. 826-836

An experimental and simulation validation of residual stress measurement for manufacturing of friction stir processing tool

Ravi Butola, Qasim Murtaza & Ranganath Muttana Singari*
Department of Mechanical Engineering, Delhi Technological University, Delhi 110 042, India

Received: 26 May 2020

Residual stresses have been considered to be an important parameter when friction stir processing (FSP) tool is to be manufactured. FSP has often been used for surface modification and fabrication of surface composites. Involuntary residual stress in a designed tool may cause it to fail before due time. Because of this, the knowledge about the stresses on the tool probe after its machining has been considered to be desirable. The present research has focused on the analysis of the residual stresses on the tip and periphery of the FSP tool probe which has been manufactured using H13 tool steel material during the turning processes on a CNC lathe machine. The experiments have been performed on two different types of tool probes, namely circular, tapered circular probes. ABAQUS/CAE simulation has been performed for circular and tapered circular probe, as the provision of a sustainable, simple and reasonable model to analyze the machining processes (using ABAQUS/CAE software) has been the primary objective of this research. The results have been found to be within a close range of the experimental observations. The same model can thus be applied to other geometries.

Keywords: ABAQUS/CAE, Residual stresses, Turning, Tool steel, Friction stir processing

1 Introduction

In the past few years, the use of high-speed steel has accelerated, owing to its high strength to weight ratio. In designing a mechanical component from raw material, many machining processes are carried out, which induce residual stresses in the component. Fatigue life is highly affected by the presence of residual stresses. FSP is an adaptation of friction stir welding (FSW), which is a solid-state joining method invented at The Welding Institute of UK in 1991. FSP is a solid state processing and is used in the microstructural modification of the surface of materials. FSP is a solid state plastic deformation method which works with the help of a rotating non-consumable tool comprising of a shoulder and a probe at the end[1,2]. Hence, it is crucial to anticipate these residual stresses so as to increase the life of the component. Various methods have been adopted in the past for measuring residual stresses in a component. These include destructive and non-destructive experiments. XRD is the most commonly used process for measurement of the residual stress. However, the initial set-up cost for XRD is very high. Since the present arena is of digital computers, in this research we have used the capabilities of a computer for determining the residual stress. Experimental analysis of surface stresses due to deformation processes such as bending and stretching was done and it was found that during machining, compressive surface residual stresses and informing operation tensile surface residual stresses are formed. They also found that increasing incremental angle results in a decrease in the compressive surface residual stresses using turning process[3]. Hard machining test was conducted on heat-treated AISI4340 steel to investigate the residual stresses and changes in the microstructure. It was suggested that good surface integrity characteristics could be attain with suitable machining parameters[4]. Temperature dissemination, bending and residual stress created during plasma arc facing over AISI4140 entryway valve was contemplated utilizing FEA. After simulation, residual stresses were analyzed and estimated by X-Ray diffraction method. Numerical outcomes demonstrated great concurrence with experimental test[5].

Research was carried out to determine the impact of preheating on microstructure, mechanical properties and stress on tool steel SLM parts. It was found that the residual stresses are compressive at low preheating temperatures and on increasing the preheating temperature, tensile nature increases[6]. Some researchers presented an illustrated review report on the

*Corresponding author (E-mail: ranganath@dce.ac.in)

machining of stimulated surface probity in titanium and nickel alloys where it was discussed about the increasing use of these alloys, impact of residual stress and surface integrity on the performance, various parameters of machining affecting the microstructure and various methods to reduce the generated residual stress during the machining process[7]. A few researchers reported the residual stress generated during the facing of high strength nickel-based superalloy RR1000 by various parameters such as type of tool, coated tool, tool wear, and failure. They obtained medium increment in tool wear leads to highest tensile surface stress, and the round insert in comparison to rhombic insert produce slightly increase in tensile stress[8]. In this work a trial and theoretical examination in regards to the impact of the working parameters on residual stress distribution created by milling. The tests are completed on carbon steel K945. The cutting system is shifted as: v=16 to 1036 m/min; f=375 to 1400 mm/min; DOC= 0.15 to 0.5mm. A small cutting depth (equivalent to 0.15 mm) created the lowest values of residual stress. The utilization of high cutting feed (equivalent to 1400 mm/min) lead to huge variations of residual stress[9]. The machining parameter and temperature throughout end milling cutting operation were investigated with various feed rates and DOC and the surface residual stress was measured along acentric direction after turning. It was found that the residual stress along an acentric direction at the middle point was tensile and the mechanical effect represented by cutting forces made the surface residual stress of compressive nature along the eccentric direction[10]. The profile was optimized along with the residual stress by analyzing the effect of DOC on the rearrangement of residual stress during milling of a thin-walled part. It was observed that the depth of cut reduced from roughing to finishing in the operation and the machined surface residual stress decreased[11]. Some researchers studied the residual stress stimulated by orthogonal cutting of tool steel by modelling and simulation using FEM. The residual stresses obtained by modelling were validated using XRD. They obtained that the surface residual stress increased and became more compressive if any of the parameters - cutting speed, uncut chip thickness and tool wear is increased[12]. A report found that the residual stress stimulated by dry turning of H13 tool steel. Residual stress was check out practically in a function of the tool geometry and machining parameter. He found that the maximum and minimum principal residual stress were of tensile and compressive nature respectively. He also found that to minimize the measure of tensile residual stress feed should be decrease and tool-cutting angle is to be increased[13]. Residual stress was analysed in the shaping of AISI 1020 steel. They compared the FEM simulation of single point cutting process with the experimental work results. XRD technique was utilizing to find out the residual stresses. Process variables were optimized using Taguchi L_9 experimental design and found that rake angle of 12°, DOC is 1 mm and cutting speed of 220 m/min was most effective in shaping[14]. Another study dissected SR on CNC turned AISI410 with various coated cutting tool under dry conditions. Multilayered coated with TiCN+Al_2O_3 of 14 μm embed is utilized for case-I, multilayered coated with Ti(C, N, B) of 6μm embed is utilized for case-II and single layered coated with (Ti, Al) N of 3 μm embed is utilized for case-III. From the outcomes of ANOVA, the feed rate and cutting velocity are the noteworthy cutting parameters for influencing the SR with Ti(C, N, B) and(Ti, Al) N. From the consequences of ANOVA, the feed rate and DOC are the significant cutting parameters for influencing the SR with TiCN+Al_2O_3[15]. Another researcher performed experiments and built the FEM model of orthogonal cutting of 316L steel. It was achieve that the experimental and FEM models gave the similar tendency of residual stresses peak profile[16]. The residual stresses on specimen surface, after cutting process was investigated using FEM modal, and the outcomes were compared with the experiments[17]. In this research, the impacts of a different cooling fluid on residual stresses were studied. To determine residual stress profiles, XRD technique was used. After experiments were performed, the FEM model was applied and compared with the experimental outcome[18]. Analyzed the residual stress in the shaping of AISI1020 and CNC turning of H13 tool steel and, then compared the FEM simulation of single point cutting process. XRD technique and PulsetecμX-360n portable stress analyzer was used to measure residual stress [19-21]. The conclusion of this research will have a large impact on the fabrication of FSW/FSP tool industry. The forecasting of residual stresses utilizing ABAQUS/CAE 6.14 software gives an opportunity to FSW/FSP tool industries to improve the machining process of FSP tool design before manufacturing the tool. The researchers have presented various ways to use computational power to find out the residual stresses in turning operation. Most of the research work is based on orthogonal cutting and are 2-D simulations. In this research, we have used the explicit dynamics of ABAQUS to simulate the oblique cutting in 3-D environments.

This research aims to find out the residual stress on the periphery and tip of the circular and taper circular FSP tool probe. The residual stresses were calculating using PulsetecμX-360n stress analyzer machine. The experiments were performed on two different types of tool probe profiles. The experimental results were compared with the outcome got from ABAQUS/CAE simulation of the turning process.

2 Experimental procedure

The material used for conducting experiments was H13 tool steel workpieces (specimen) dimensions 100xØ22 mm as shown in Fig. 1(a) were used in this investigation. In this study, two work pieces were made with following different probe profile, circular, tapered circular. Machining was carried out on the CNC Lathe machine set up with the carbide insert as shown in Fig. 1(b). Feed rate and cutting speeds were 0.15 mm/rev and 1500 m/min respectively. The circular and taper circular probes were generated in 2 steps turning from an initial 22 mm diameter rod. In the first part of the turning process, the dia was reduced from 22 mm to 19.95 mm for the complete length of the specimen. In the second part, diameter decreased from 19.65 mm to 7.22 mm for a probe length of 3.5 mm. The taper circular probe was fabricated by using a taper turning attachment and a taper of length 3.5 mm was generated with the diameter gradually decreases from 7.22 mm to 3.5mm. After the completion of the machining process of H13 tool steel, the residual stresses on the machined work pieces was determined.

2.1 Measurement condition

Residual stresses were measured in two different probes with a portable stress analyzer. For each work piece, two tests were done on the circular probe and taper circular probe periphery. Following are the measurement conditions for analysis of residual stress in two different probes are: X-ray tube current = 1.00 mA, voltage = 30 kV, incidence angle = 35°, wavelength (K-Alpha) = 2.29093[A](Cr), wavelength (K-Beta) = 2.08480[A](Cr), temperature = 34.81 °C.

2.2 Set-up and methodology

In this investigation, residual stresses were estimated utilizing PulsetecμX-360n portable stress analyzer machine set up as shown in Fig. 2(a-c). These readings were then contrasted and the outcomes got from ABAQUS/CAE simulation of the turning process. The specifications of the machine are maximum measurement distance = 51 mm, X-Ray tube voltage & current = 30KV/15 mA max, measurement method = Single incident angle method (cosα method), measurement time = 60 sec, target material = Ferrite, aluminium, nickel, titanium, ceramics etc. This machine uses cosα method for determining the residual stress. The cosα technique is as promising as $\sin^2\Psi$ technique and with similar errors. However, $\sin^2\Psi$ is the time intensive method and requires a full X-Ray diffractometer setup.

2.3 Residual stress measurement of FSP tool probe

The residual stress measurement was done on the specimen, which was made of tool steel material utilizing Pulsetecμ X-360n stress analyzer machine. Two tests, i.e. TEST 1 and TEST 2, were performed on the periphery and the probe tip of the circular probe, while TEST 3 and TEST 4 were performed on the periphery and the probe tip of taper circular probe. The measurements were done by cosα method consisting of a gyro sensor for displaying the sensor unit angle. The value of diffraction angle 2θ = 156.396 degree, Diffraction lattice angle = 23.604 degree, interplanar spacing(d) = 1.170, plane(h,k,l) = 2,1,1, crystal structure = BCC, young modulus(E) = 224 GPa, Poisson ratio(v) = 0.280 were taken during measurement.

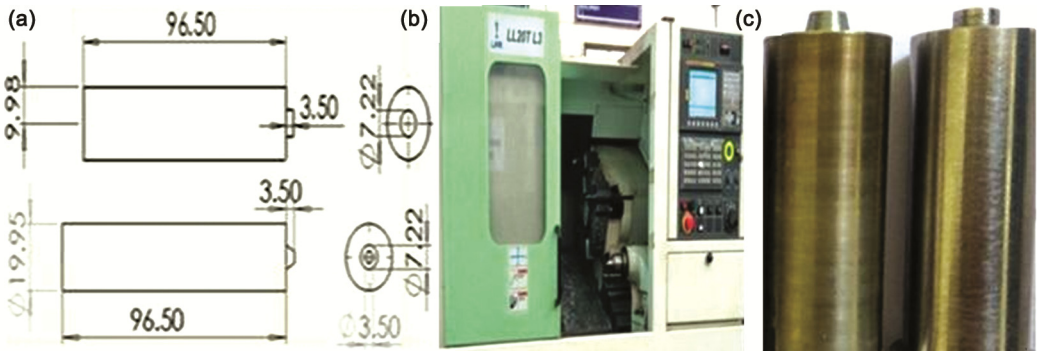

Fig. 1 — (a) Dimension of tool and (b) CNC lathe machine set up.

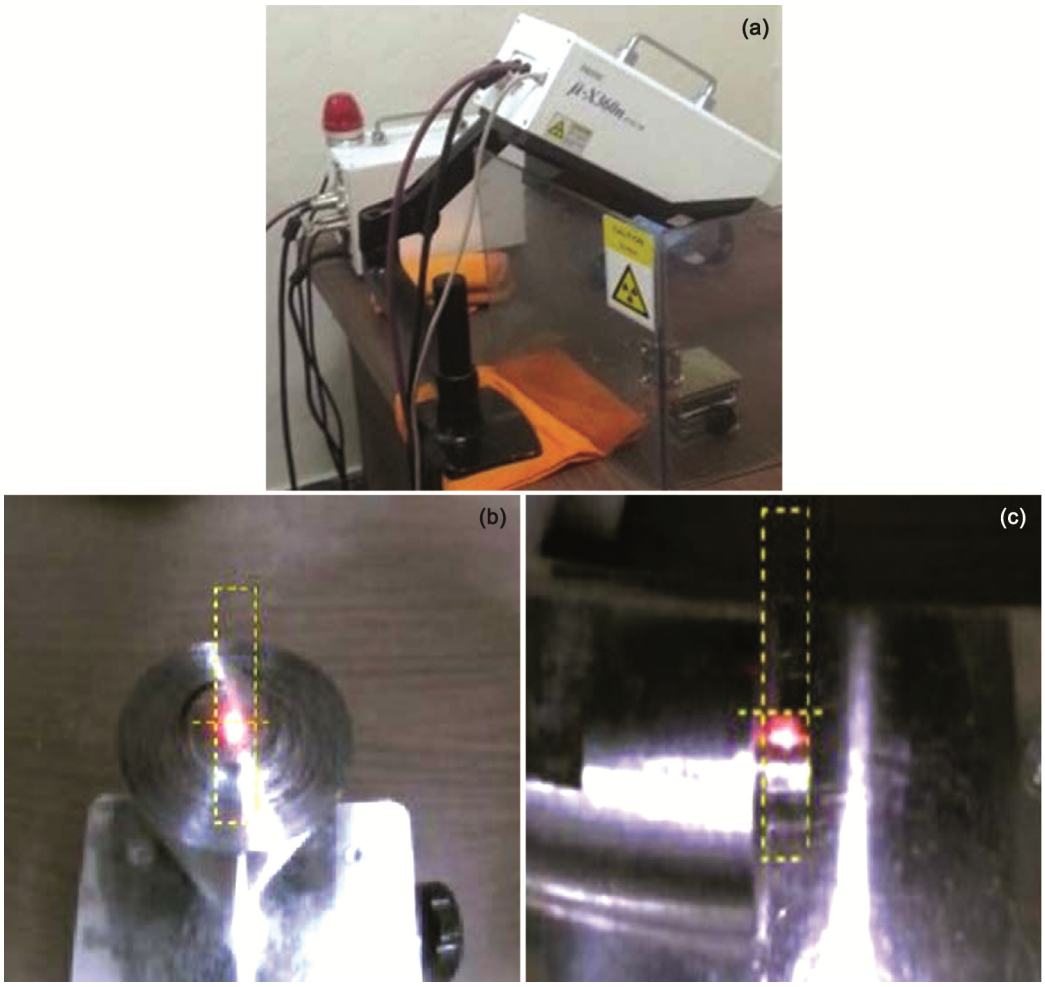

Fig. 2 — (a) Portable stress analyzer setup, (b) Image captured in circular probe and (c) Taper circular probe.

3 Turning simulations

Turning process on lathe machine involves oblique cutting and chip formation. It's therefore, a very complex machining process and so, research is still going on in the search for a formalized methodology to completely simulate the cutting process. The difficulty arises due to the multiple cutting forces involved, the chip formation, temperature changes, varying shear deformation zones and many such factors. Since we need to find out the residual stresses in the H13 tool steel workpiece after it's turned on the CNC lathe machine by a single point cutting tool of carbide insert, naturally, multiple time steps must be input along with a precise degree of mesh accuracy and computational power.

In the Materials module, the material is characterized by adding the properties of specimen, for example, types of material. In the material practices segment properties like conductivity, ductile damage, Shear damage with damage evolution, density, elastic, thermo-viscoplastic properties are characterized. In the current study, Johnson-Cook damage criterion was utilized. In the mesh module, 3D Stress group of explicit, linear geometric order, hex element type was designate to the specimen. Element deletion was picked since we were not intrigued by chip stream and only the stresses on the specimen. In the interaction module, Friction contact with the coefficient of 0.4 was utilized. Another material was defined with a density of 100000, a Young's modulus of $1 \times e^{+20}$ and Poisson's ratio of $1\times e^{-6}$. This material was assigned to the cutting tool to approximate the behaviour of a rigid tool since we are not interested in the residual stresses or deformations in the cutting tool.

3.1 Modeling of circular and taper circular FSP tool probe

Finite element analysis (FEA) is the modeling of the turning process to create a tapered probe tool.

A round sketch of 22 mm range and 30mm deep was drawn. This was raw component of the specimen. Figure 3(a&b) shows the geometry of workpiece radius 22 mm and workpiece was extruded to 30 mm deep. It is not exactly the definite length of the specimen since we are just intrigued by the part which is close to the periphery and tip of the tool probe. This assumption is reasonable and spares a considerable amount of meshing and computational time. Figure 3(c&d) shows the partitioned regions in the work piece and a simple single-point cutting tool is generated. This helps, bettering the mesh quality. Since there was step turning included, various parts can be meshed to be of better/coarser quality. A reference point (RP) was also added to the center of the face. Figure 4 (a&b) the material was assigned to the cutting tool to approximate the behavior of a rigid tool since we were not interested in the residual stresses or deformations in the cutting tool. The parts are assembled in the Assembly module. A small gap of 0.5 mm between the cutting tool and the specimen is given. Figure 4 (c&d) shows the Interaction module, Surface-to-surface contact is selected between the tool and workpiece. Friction contact with the coefficient of 0.4 was used. Constraints are added of coupling type to the tool and the workpiece, coupled with their respective reference points. A rigid body coupling is also given to the tool. Figure 5 (a&b) shows the stress analysis of the circular tool probe, in the load module where the limit conditions are altered, with the goal that the tool traverses in a straight way laterally to the specimen axis.

Figure 5 (c&d) shows the stress examination of the taper circular tool probe profile test was like the strategy depicted in the past segment. The main special case i.e., in the load module, boundary conditions are entering. Here, the angular velocity to the specimen, the feed rate and DOC is given to the cutting tool.

4 Results and Discussion

Estimation of residual stress due to machining would now be able to be envisioned through simulations as a result of advancements in technology and various ways to use computational power to regulate the residual stresses in turning operation. Most of the research work is based on orthogonal cutting and are 2-D simulations. In this research, we have used ABAQUS explicit dynamics to simulate the oblique cutting in 3-D environments. After turning process completed the next step is to residual stress measurement of machined specimen. Residual stresses data was obtained by utilizing a PulsetecμX-360n stress analyzer machine. A procedure for simulation is formulated which can be applied to similar machining processes. Various manufacturing operations that transform the shape or change the characteristics of the materials such as deformation of the material, machining operations or other processes contribute to the generation of residual stresses. These can be achieve in a material which has not gone through any

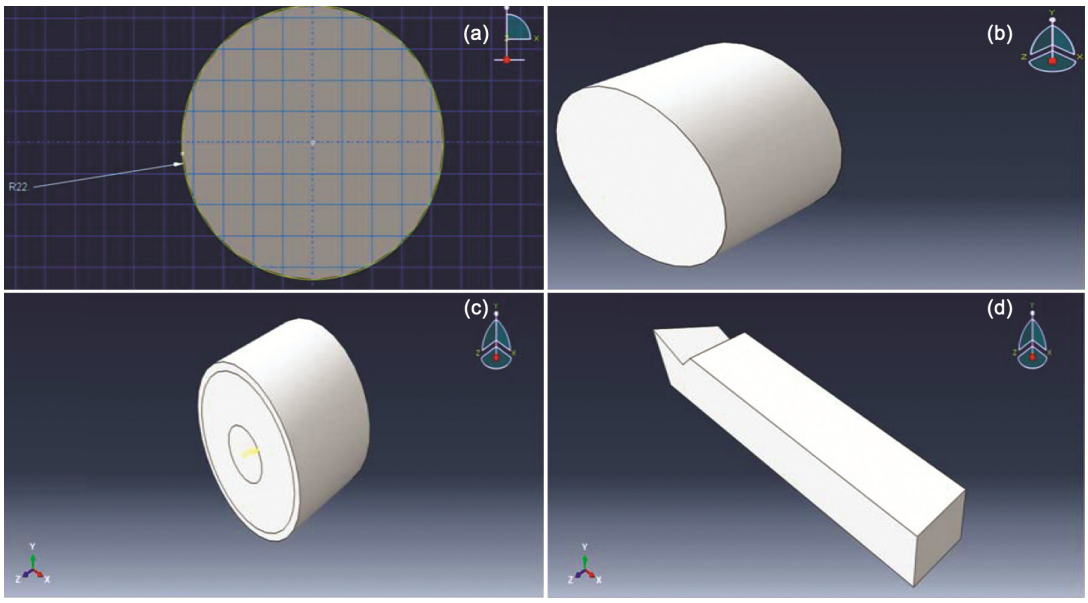

Fig. 3 — (a) Geometry of workpiece R22 mm, (b) Extruded cylinder workpiece 30 mm, (c) Partitioned regions in the work piece and (d) Single point-cutting tool.

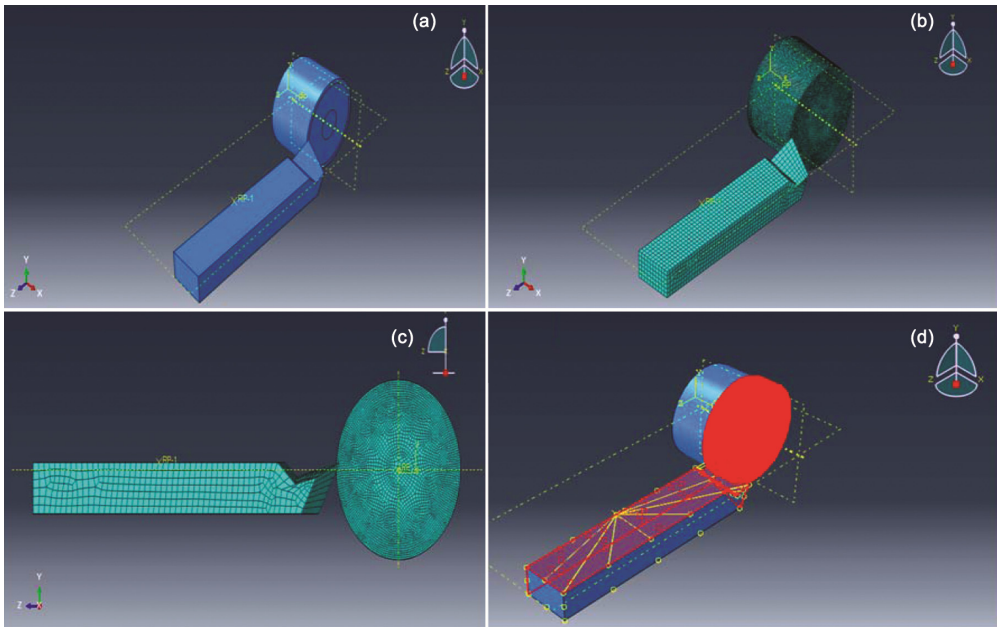

Fig. 4 — (a) Assembly, (b) Meshing top view, (c) Meshing front view and (d) Surface to surface contact.

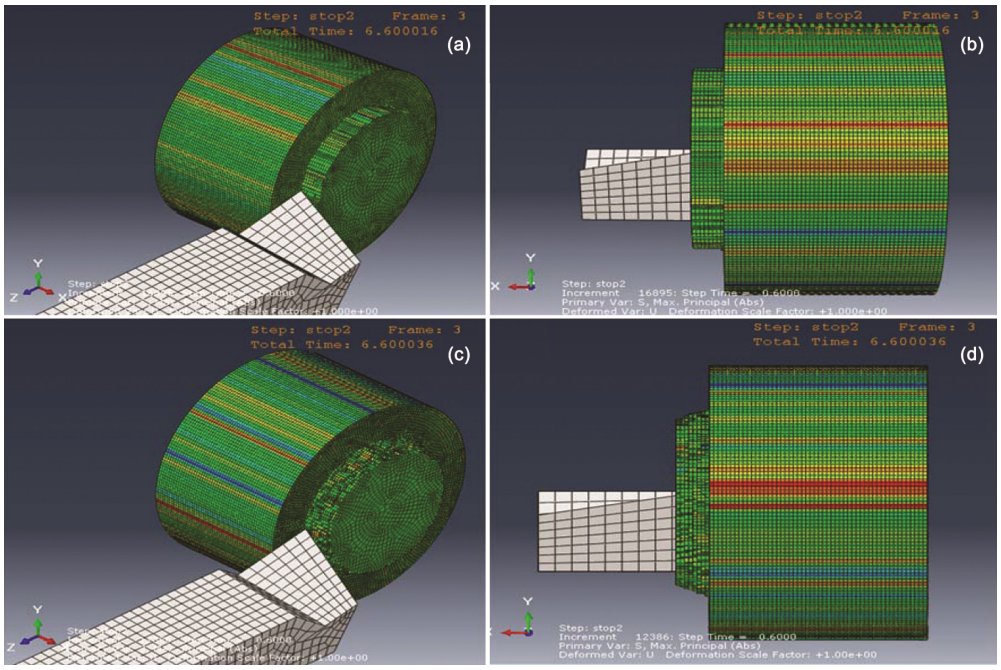

Fig. 5 — Machining visualized with stress contours of (a, b) Circular probe and (c, d) Tapered circular probe.

process, as it depends on various factors and may get generated during manufacturing and operational conditions[22]. Residual stresses may be present on the micro-level and on the macroscopic level. They tend to affect the performance of that material, as it can cause local yielding or plastic deformation. Hence, measurement and analysis of this residual stress in the components becomes vital.

Friction stir processing tool, which was manufactured by H13 tool steel material, plays an important role in friction stir processing. It decides what kinds of materials could be processed and the dimension of the workpiece. The shoulder controls the material flow in a certain region, and the probe generates heat and severe plastic deformation. Eventually, the friction stir tool affects the microstructure and mechanical

properties. However, little knowledge about the friction stir processing tool geometry was published before, and information on friction stir welding tool could be a reference to understand the tool[23-25]. The result of Test 1 and Test 2 sample of residual stress on the probe periphery and tip of the circular probe was found to be compressive 139 MPa and 109 MPa with a S.D of 9 MPa and 14 MPa respectively. The result of Test 3 and Test 4 sample of Residual Stress on the probe periphery and tip of tapered circular probe was found to be compressive 199 MPa and 175 MPa with a S.D of 11 and 17 MPa, respectively.

The scattered X-rays were recorded for a family of planes {h,k,l} and using Bragg's law lattice spacing can be found then strain[26] is obtained by Eq. (1):

$$\varepsilon_{\varphi\Psi} = \frac{d_{\varphi\Psi} - d_0}{d_0} \quad \ldots (1)$$

where, $\varepsilon_{\varphi\Psi}$ is the calculated strain for the {h,k,l} planes for a sample orientation referred by the φ and ψ angles, and d_o is lattice spacing for an unstressed sample**.** In fact, the strain varies with the ψ angle along the normal to the diffraction plane[27]. Equation (2) expresses the $\varepsilon_{\alpha,}$ the parameter used to calculate the stress[28].

$$\underline{\varepsilon}_{\alpha}^{\{hkl\}} = \frac{1}{2}\left[\left(\varepsilon_{\alpha}^{\{hkl\}} - \varepsilon_{\pi+\alpha}^{\{hkl\}}\right) + \left(\varepsilon_{-\alpha}^{\{hkl\}} - \varepsilon\pi - \alpha hkl\right)\right. \quad \ldots (2)$$

where, ε_{α}, $\varepsilon_{\pi+\alpha}$, $\varepsilon_{\pi-\alpha}$, $\varepsilon_{-\alpha}$ are strains determined at four points located at 90 degree on the Debye ring. Equation (2) provides the stress for the cosα method:

$$\sigma_{\varphi} = \frac{E^{\{hkl\}}}{1+v^{\{hkl\}}} \frac{1}{sin2\eta sin2\Psi_0} \frac{\partial \underline{\varepsilon}_{\alpha}^{\{hkl\}}}{\partial cos\alpha} = \frac{1}{\frac{1}{2}S_2^{\{hkl\}}} \frac{1}{sin2\eta sin2\Psi_0} \frac{\partial \underline{\varepsilon}_{\alpha}^{\{hkl\}}}{\partial cos\alpha} \quad \ldots (3)$$

Figures (6-9) residual stress graphs represent the variation of the parameter a_1 and a_2, which are used for the linear determination of σ_x and T_{xy}, respectively. Following equations represent the variation of a_1 and a_2 with cosα and sinα, respectively.

$$a_1 = \frac{1+v}{E}\,\sigma_{11} sin2\Psi_0\, sin2\eta\, cos\alpha \quad \ldots (4)$$

$$a_2 = 2\frac{1+v}{E}\,\sigma_{12} sin\Psi_0\, sin2\eta\, sin\alpha \quad \ldots (5)$$

The red line in the above graphs represents the average value of parameters a_1 and a_2 when α varies from 0 to 90 degree. A good linear behavior has been obtained between parameter a_1 and a_2 and angle α as shown in Figs (6-9).

From Fig. 10(a) the variation of absolute residual stress versus time for circular probe and it can be noticed that residual stress at the probe tip increase in both the cases with machining time. Figure 10(b) shows the variation of absolute residual stress versus time in the tapered cylinder probe tip in the second pass turning operation. Here the variation is taken from t = 6s to t = 7s, *i.e.* the time for the second pass of turning is 1 sec in the simulation. Similarly as shown in Fig. 10 (a&b) shows that more residual stresses are

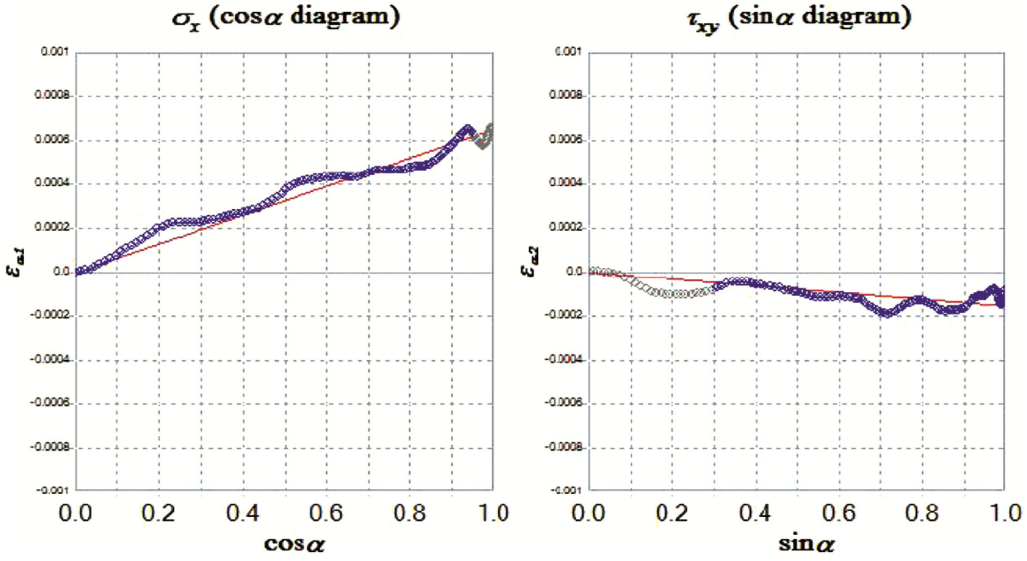

Fig. 6 — Residual stress graph circular probe (Test 1).

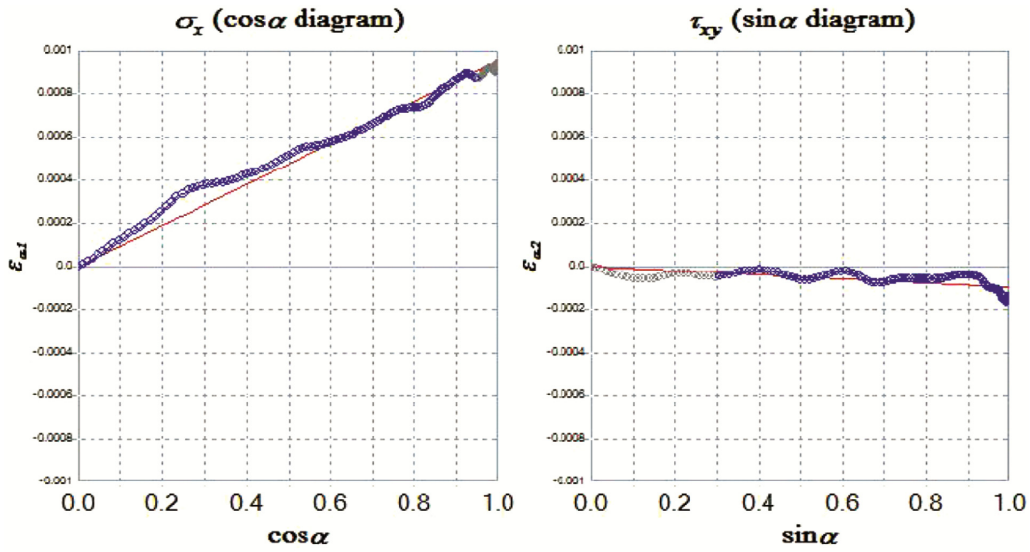

Fig. 7 — Residual stress graph circular probe (Test 2).

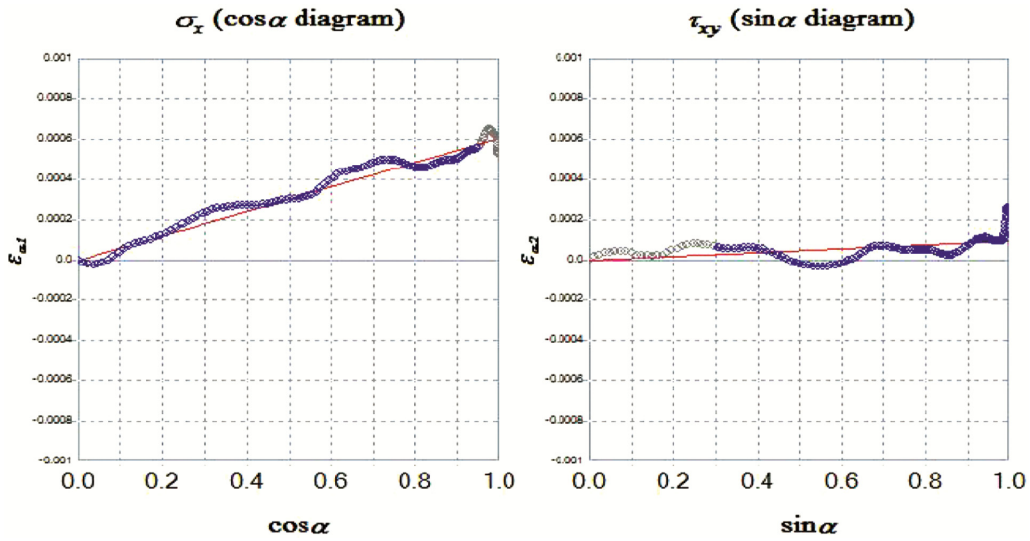

Fig. 8 — Residual stress graph tapered circular probe (Test 3).

generated in tapered circular probe profiles, which can be understood from the fact that in turning the probe profile, the diameter of the tapered probe is less at the tip in comparison to the diameter of the tip of a circular probe. In tapered machining, material removal rate decreased from small diameter end to large dia end of the probe because of which the variation in residual stress in the tapered probe is less as compared to the variation of residual stress in the circular probe.

A comparison in the form of a histogram is presented in Fig. 11 that depicts the residual stresses in different probe profile. It is evident that maximum stress was obtained in taper circular probe profile and the minimum in circular probe profile. The reason for this variation of residual stress was due to the type of machining done in the different specimen. As a result of this, taper circular probe profile faces maximum residual stress. In circular probe profile, only turning was done. But in tapered circular, the diameter was the same as that of the cylinder on one side and less on another side. For the tapered probe, more machining was required than the circular probe. Hence, more residual stresses were induced in the tapered circular probe profile.

5 Validation of experimental and simulation work

Before residual stresses measurement was done on the workpiece surface, the machining parameters and

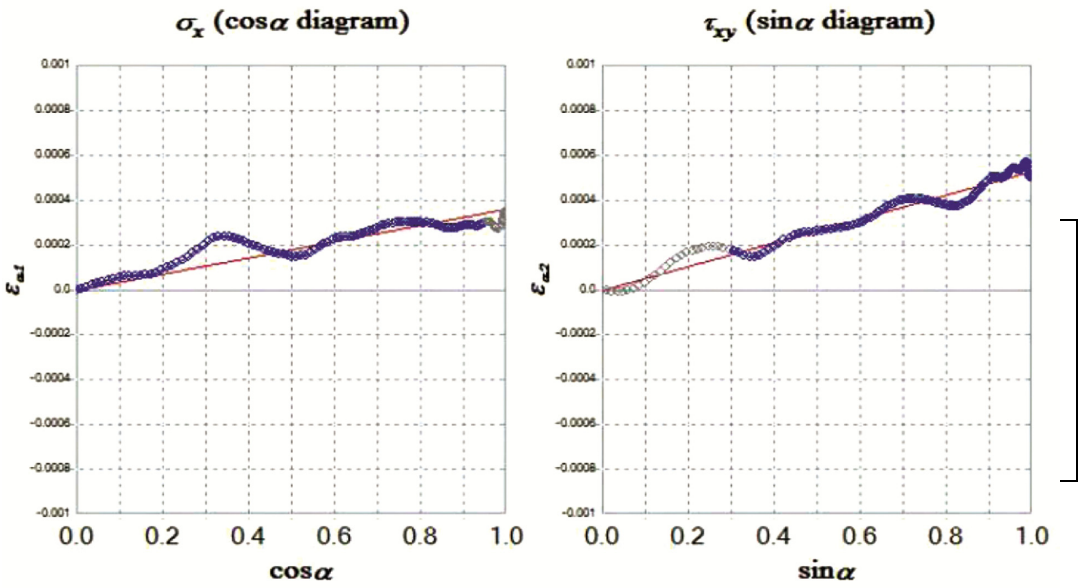

Fig. 9 — Residual stress graph tapered circular probe (Test 4).

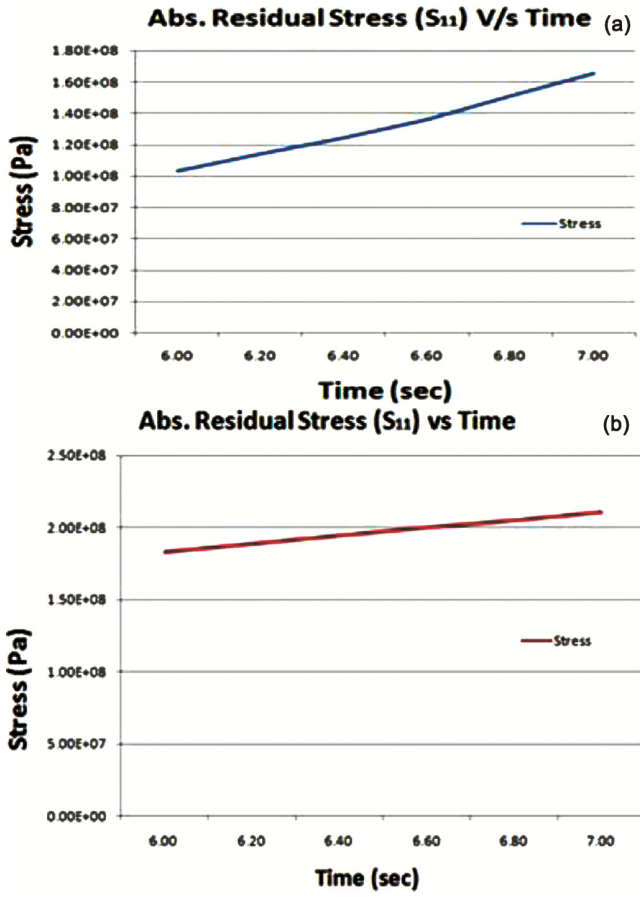

Fig. 10 — Residual Stress versus time for probe tip (a) Circular probe and (b) Taper circular probe.

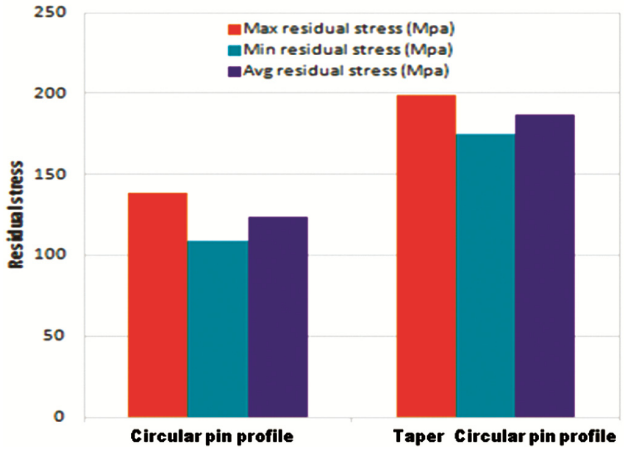

Fig. 11 — Comparison of residual stress on different probe profile.

Abaqus/CAE simulation were observed. The experiment and simulation results for the machining parameter and the residual stresses were compared and are a strong testimony for the validation of the current model. From X-Ray stress analyzer of residual stress in machining, different probe profile developed a residual stress and the values are given in Table 1.

From the Fig. 12, residual stress verses time graphs, obtained from ABAQUS/ CAE simulation, we can infer that stress is found to increase during the turning process and the increase is linear in both cases. For the circular probe, the average residual stress is found from simulation to be compressive 130 MPa approximately. This suggests compressive stress on the probe periphery. From experimental readings,

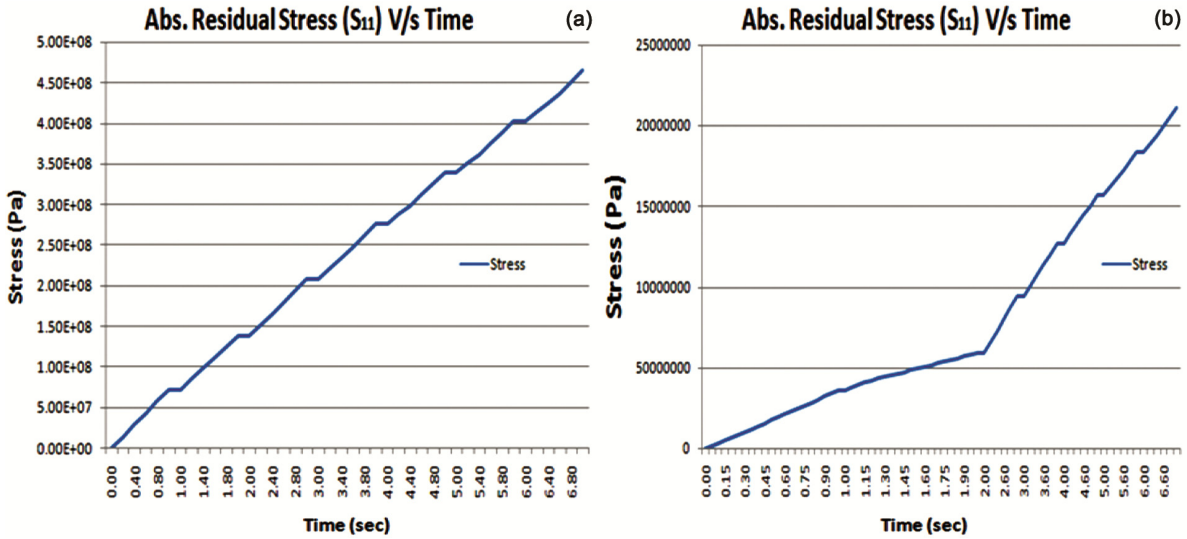

Fig. 12 — Residual stress versus time for probe periphery (a) Circular probe and (b) Taper circular probe.

Table 1 — Residual stress in different probe profile.

S.No.	Probe Profiles	Absolute residual Stress [MPa]	Average residual Stress [MPa]
1	Circular	109	124
2	Circular	139	
3	Tapered Circular	175	187
4	Tapered Circular	199	

the average residual stress was found out compressive 124 MPa. So the percent error is 8.06%. For the tapered circular probe, the average residual stress is found from simulation to be compressive 199 MPa approximately. This indicates compressive stress on the probe periphery. From experimental readings, the average residual stress was found out compressive 187 MPa. So the percent error is 6.41%.

Since the error value is found to be within an acceptable range, it can be concluded that the experimental readings obtained for the circular and tapered circular tool probe complement the FEA model simulation results.

6 Conclusions

In the current research work, an experimental and simulation study was carried out on residual stresses developed due to the machining of H13 tool steel. The specimens were made in the shape of FSP tool with two different probes, *i.e.* circular and taper circular. The conclusions made from this study are as follows:

(i) The residual stress measured by X-Ray stress analyzer was found to be maximum in a tapered circular and least in circular probe profile. This can be attributed to the fact that more machining processes were done in tapered circular probe in comparison to cylinder probe. The difference in residual Stress between the cylinder probe and Taper cylinder probe as analyzed by X-Ray stress Analyzer was 53 MPa.

(ii) Successful simulation of turning process was carried out in Abaqus/CAE software. Demonstration of oblique cutting in simulation was done successfully.

(iii) Experimental readings validate the simulation results for the tapered circular and circular probe with the error values lying in an acceptable range. The errors can be minimized by improving the mesh quality. The difference in residual stress in cylinder and the tapered circular probe as analyzed by simulation in ABAQUS was 65 MPa.

References

1 Mishra R S & Ma Z Y, *Mater Sci Eng R Rep*, 50 (2005) 1.
2 Butola R, Ranganath M S & Murtaza Q, *Eng Res Express,* 1 (2019) 025015.
3 Singh A & Agrawal A, *J Mater Process Technol*, 225 (2015) 195.
4 Jomaa W, Songmene V & Bocher P, *Mater Manuf Process,* 31(2015) 838.
5 Punitharani K, Murugan N & Sivagami S M, *J Sci Indust Rese*, 69 (2010) 129.
6 Mertens R, vrencken B, Holmstock N, Kinds Y, Kruth J P, Humbeeck J V, *9th Int Conf Photon Technol-LANE*, (2016) 882.
7 Ulutan D & Ozel T, *Int J Mach Tools Manuf*, 51 (2011) 250.
8 Li W, Withers P J, Axinte D, Preuss M & Andrews P, *J Mater Process Technol,* 209 (2009) 4896.

9 Tâmpu N C, Chiriţă B, Herghelegiu E & Brabie G, *Indian J Eng Mater Sci,* 21 (2014) 283.
10 Maa Y, Fenga P, Zhanga J, Wua Z & Yua D, *J Mater Process Technol,* 235 (2016) 41.
11 Beizhi Li, Jianga X, Yanga J & Steven Y L, *J Mater Process Technol*, 216 (2015) 223.
12 Caruso S, Outeiro J C, Umbrello D & Saoubi R M, *J Mater Form*, 31 (2010) 515.
13 Outeiro J C, Machines et Usinage à Grande Vitesse (MUGV), *ENISE–CETIM, Saint-Etienne*, October (2012), France.
14 Bhatkar O, Sakharkar S, Mohan V & Pawade R, *Adv Intell Sys Res,*137 (2017) 100.
15 Chandrasekaran K, Marimuthu P, Raja K & Manimaran A, *Indian J Eng Mater Sci,* 20 (2013) 398.
16 Outeiro J C, Umbrello D & Saoubi R, *Int J Mach Tools Manuf*, 46 (2006) 1786.
17 Attanasio A, Ceretti E & Giardini C, *Mach Sci Technol*, 13(2009) 317.
18 Hribersek M, Pusavec F, Rech J & Kopac J, *Mach Sci Technol*, 22 (2018) 1.
19 Butola R, Kumar J, Khanna V, Ali P & Khanna V, *Mater Today: Proc*, 4 (2017) 7892.
20 Butola R, Murtaza Q & Singari R M, *Lecture Notes on Multidisciplinary Industrial Engineering, Springer* (2019) 337.
21 Bhatkar O, Sakharkar S, Mohan V & Pawade R, *Adv Intell Sys Res,* 137 (2017) 100.
22 Withers P J & Bhadeshia H K D H, *Mater Sci Technol*, 17 (2001) 366.
23 Thomas W M, Johnson K I & Wiesner C S, *Adv Eng Mater*, 5 (2003) 485.
24 Chaudhary A, Dev A K, Goel A, Butola R & Ranganath M S, *Mater Today: Proc,* 5 (2018) 5553.
25 Zhao Y, Lin S, Wu L & Qu F, *Mater Lett*, 59 (2005) 2948.
26 Prevéy P S, *ASM Inter*, 10(1986) 380.
27 Cullity B D, Addison Wesley, *Reading, MA*, (1978) 451.
28 Tanaka K and Akiniwa Y, *JSME Int J Series A*, 47 (2004) 252.